JOURNAL OF THEORETICAL
AND APPLIED MECHANICS
3, 40, 2002

PARAMETRIC IDENTIFICATION OF MR LINEAR AUTOMOTIVE SIZE DAMPER

BOGDAN SAPIŃSKI

Department of Process Control, University of Mining and Metallurgy
e-mail: deep@uci.agh.edu.pl

The paper deals with the problem of parametric identification of phenomenological models of a MR damper. The rheological structures of the MR damper described by two fundamentals parametric models that are due to Bingham and Spencer are reviewed. The problem of identification is considered, exemplary results of MR damper experimental tests and an adjustment procedure of the estimated parameters with respect to experimental data are discussed. A linear MR damper of RD-1005 series developed by Lord Corporation has been tested and modelled.

Key words: MR fluid, MR damper, rheological structure, identification, verification

1. Introduction

There are two methods of formulating mathematical models, namely the modelling and the identification (Soderstrom and Stoica, 1997). The former uses an analytical approach and derives the system dynamics from laws of physics. The latter uses an experimental approach by fitting the system parameters to experimental data obtained for the system under investigation. For practical reasons, a stationary system is often assumed to approximate the system dynamics with a system of differential or difference equations. Thus, the parametric identification consists in determining the coefficients of system equations, while the verification reduces to resolution whether the obtained model is consistent with experimental data or not.

In this paper MR damper parametric models based on assumed rheological structures are subjected to identification. These dampers are of particular interest mainly due to phenomenological reasons (Ahmadian, 1999; Carlson

and Spronston, 2000; Chang and Roschke, 1998; Lederer et al., 2000; Li et al., 2000; Schurter and Roschke, 2000; Stanway et al., 2000; Sunakoda et al., 2000). This results from their high nonlinearity under operational conditions. An MR fluid manifests hysteresis and jump-type behaviour depending on velocity. An example of such a phenomenon is presented in Fig. 1 for a MR damper of low efficiency. The relationship between the damping force and velocity clearly indicates that for lower velocities (up to several dozens of 10^{-3} m/s) the hysteresis nonlinearity predominates (see Fig. 1a), while jump-type nonlinearity prevails for higher velocities (Fig. 1b). Such nonlinear behaviour could complicate construction of phenomenological models and reduce their applicability. There are no doubts however, that it is necessary to use promising features of MR dampers such as quick response to command signal changes, full reflexivity of MR fluid transformation and low power demand, which indicate potential applications to vibration control in dynamic structures (Carlson and Spronston, 2000; Spencer et al., 1998).

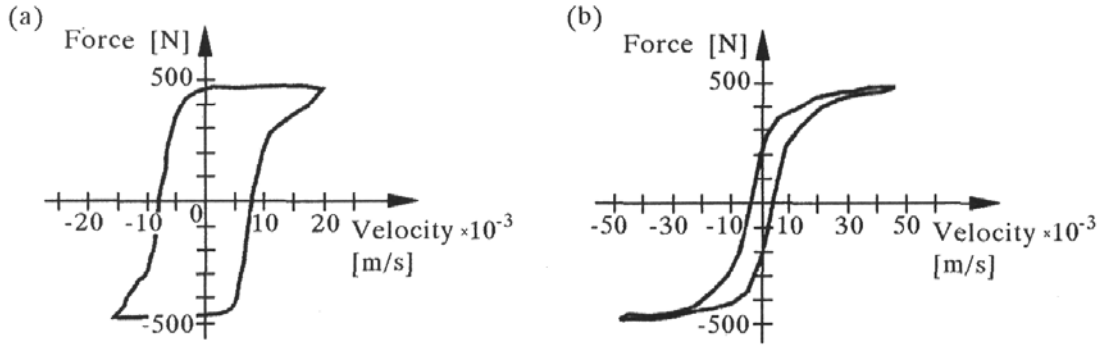

Fig. 1. Force vs. velocity at: (a) lower velocities, (b) higher velocities

An analytical approach to modelling has been proposed (Dyke et al., 1996) by presenting four parametric models for MR dampers denoted by: Bingham, Gamota-Fillisko, Bouc-Wen and Spencer. These models differ in the adopted rheological structure and allow one to predict the MR damper behaviour at various accuracy levels. The Spencer model has been extended (Li et al., 2000) by using viscoelastic-plastic model of the rheological structure developed by Kamath and Wereley (1997) for MR dampers. That model provides good approximation of MR damper behaviour at higher excitation frequencies. There is also a nonparametric approach to modelling of MR linear dampers. Appropriately chosen functions (polynomials, hyperbolic tangent, delay etc.) as well as fuzzy logic and neural networks were used by Ahmadian (1999), Schurter and Roschke (2000), Chang and Roschke (1998), respectively.

An attempt to estimate the model parameters was made in a number of papers. In these papers a MR damper of parameters close to those of the analysed damper was considered. An analysis by Grzesikiewicz et al. (1999) was constrained to presentation of model parameters fit to experimental data only for sinusoidal kinematic excitation of $10 \cdot 10^{-3}$ m in amplitude and 2 Hz in frequency and a control current of 3 A, when using the standard visual compatibility criterion. Similar analysis was carried out (Li et al., 2000) for several values of kinematic excitation and control current to evaluate the model parameters, but the visual fit criterion was used for the damping force vs. time relationship only. The dependence of certain system parameters on the control current was taken into account (Dyke et al., 1996) and then the parameters were fitted to experimental data (by using normalised weighted errors for the force vs. time, force vs. displacement and force vs. velocity relationships as a fit criterion). The results obtained only for sinusoidal kinematic excitation of $15 \cdot 10^{-3}$ m in amplitude and 2.5 Hz in frequency and a control current corresponding to the voltage signal of 1.5 V were presented.

When analysing the results by Sapiński (2001a,b) and the approach to model the parameters fitting MR dampers in the papers mentioned above, it seems that the identification difficulties originated from hysteresis and jump-type nonlinearity, on the one hand, and limitations of the testing machines, on the other. The latter consists in ability to achieve larger amplitudes at higher kinematic exciting frequencies. The aim of this paper is to carry out parametric identification for MR damper linear models in response to the problems mentioned above and encountered by the author while analysing experimental data.

2. Description of the MR damper

The simplified diagram of a structure of a low efficiency MR linear damper is shown in Fig. 2. The damper of a cylindrical shape is filled in with a sort of MR fluid. The magnetic field excited in the damper is generated by the control current I in the coil incorporated in the piston. The design of the piston with the coil integrated ensures that the magnetic field is focused within the gap, i. e., inside a volume of the active portion of the MR fluid.

The MR damper operation is based on the so-called MR effect (Kordoński, 1993), whose most significant feature is the change of fluid viscosity within a time of milliseconds. As a result, the MR fluid flow through the gap is restricted, and in consequence, hydraulic resistance against the piston displacement

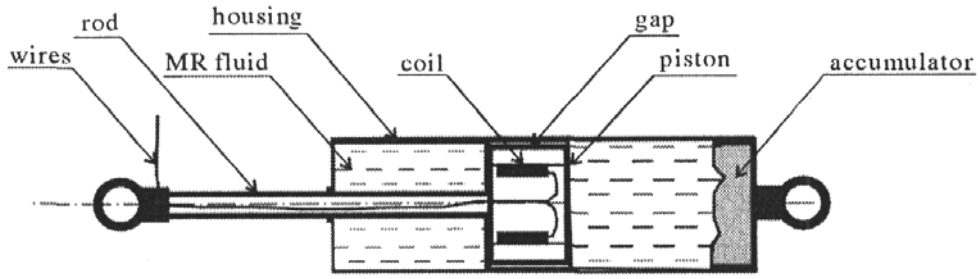

Fig. 2. Simplified diagram of MR linear damper

increases. Finally, the damping force of appropriate magnitude is generated. In the absence of the magnetic field $I = 0 \Rightarrow H = 0$, ferromagnetic particles are suspended in the carrier fluid (Fig. 3a), and in the presence of the external field $I \neq 0 \Rightarrow H \neq 0$, the particles form chain-like structures parallel to field lines (perpendicular to the fluid flow direction), thereby increasing the fluid viscosity and restricting its motion.

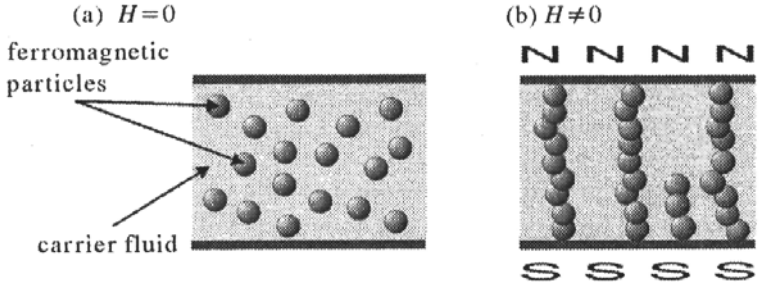

Fig. 3. MR fluid behaviour: (a) $H = 0$, (b) $H \neq 0$

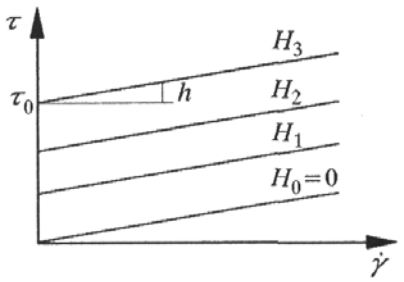

Fig. 4. Shear stress vs. shear strain rate $H_0 < H_1 < H_2 < H_3$

The stress-strain behaviour of the MR fluid is often described by the Bingham model. In this model, the MR fluid plastic viscosity η is determined

by a relationship of shear stress τ vs. shear strain rate $\dot{\gamma}$, as shown in Fig. 3. Thus, the total shear stress in the MR fluid is given by

$$\tau = \tau_0(H) + \eta\dot{\gamma} \tag{2.1}$$

where $\tau_0(H)$ is the yield stress induced by the magnetic field strength H.

3. Parametric models

Two parametric models, i.e. models by Bingham and Spencer, are taken into further considerations. These models are formulated on the basis of rheological structures for which the actual relationship between the damping force and piston velocity is approximated by characteristics presented in Fig. 5a for the Bingham model, and in Fig. 5b for the Spencer model, respectively. These two models allow one to predict MR damper behaviour with a different accuracy.

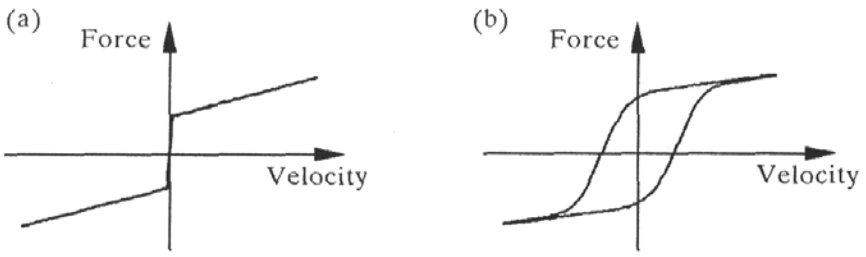

Fig. 5. Force vs. velocity for: (a) Bingham model, (b) Spencer model

3.1. Bingham model

The idealized viscoplastic, denoted by Bingham, model of the MR damper (Stanway et al., 2000) is based on both electrorheological (ER) damper model (Kamath and Werely, 1997) and similarity in rheological behaviour of ER and MR fluids. The rheological structure of the Bingham model is composed of two elements: a Coulomb friction slider and a dashpot connected in parallel, as shown in Fig. 6a. The assumed structure is different from the Bingham system as it introducies the force of a constant value f_0 that replaces the spring action.

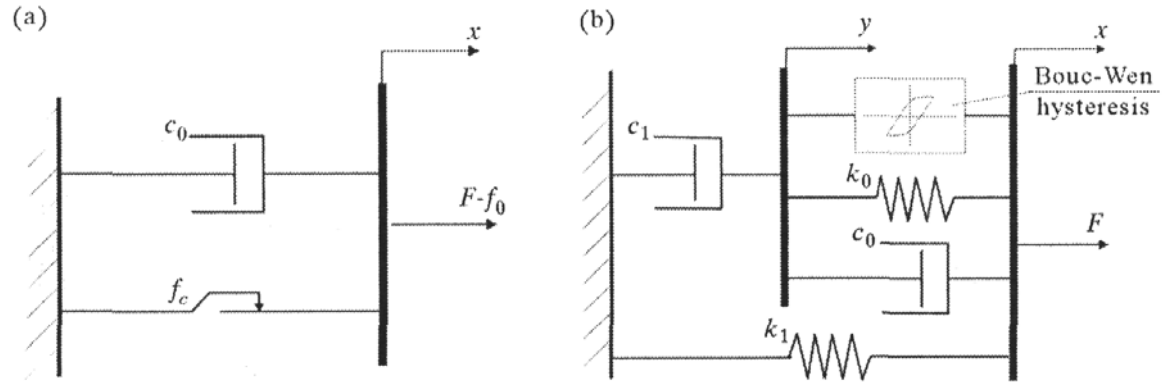

Fig. 6. Rheological structure of the MR damper for: (a) Bingham model, (b) Spencer model

The total damping force F predicted by the Bingham model for nonzero piston velocity $\dot{x}$, can be written as

$$F = f_c \operatorname{sgn} \dot{x} + c_0 \dot{x} + f_0 \tag{3.1}$$

where

- f_c – frictional force
- c_0 – viscous damping parameter
- f_0 – force due to presence of the accumulator.

The first term represents Coulomb friction mechanisms, the second one is related to the fluid yield stress and the third is an offset in the force that is accounted for the nonzero mean of the measured force value. The advantage of the Bingham model lies in its simplicity but its disadvantage consists in that if at any point the velocity of the piston is zero, the force generated in the frictional element is equal to the force applied.

3.2. Spencer model

As could be expected, the rheological structure assumed in the Bingham model exhibits some deviations from real behaviour of a MR damper. This is because that structure does not capture all significant phenomena over the whole range of the MR damper operational conditions that were observed in experimental investigations. It seems that there are two strongly nonlinear features of key significance, which should be accounted for in the MR damper model. They are related to two nonlinear phenomena: hysteretic and jump-type behaviour that may be an issue in modelling. In hysteric systems subjected to dynamic loading, the restoring force depends not only on the

instantaneous displacement but also on what happened before (previous conditions). According to the approach (Wen, 1976), based on Markov's vector formulation, the restoring force $Q(x, \dot{x})$ is assumed to have two components, one with the hysteresis $h(x)$, and the second free of it $g(x, \dot{x})$

$$Q(x, \dot{x}) = g(x, \dot{x}) + h(x) + ... \tag{3.2}$$

The $h(x)$ component is determined by equations that should be satisfied for the displacements x and h. The form of these equations depends on the number of n. If n is an odd number then the equation takes the form

$$\dot{h} = -\alpha|\dot{x}|h^n - \beta\dot{x}|h^n| + A\dot{x} \tag{3.3}$$

and if n is an even number, then

$$\dot{h} = -\alpha|\dot{x}|h^{n-1} - \beta\dot{x}h^n + A\dot{x} \tag{3.4}$$

It was shown by Spencer et al. (1998) that a good adjustment of model parameters to experimental data can be achieved for $n = 2$. This finding has been confirmed in computations carried out for the purpose of the present study. The parametric model, in which Wen's method was employed to hysteretic modelling, was introduced by Bouc-Wen (Dyke et al., 1996), and extended by Spencer afterwards. The rheological structure connected with the model is shown in Fig. 6b. The total damping force F predicted by the Spencer model can be written as

$$F = az + c_0(\dot{x} - \dot{y}) + k_0(x - y) + k_1(x - x_0) \tag{3.5}$$

or in an equivalent form

$$F = c_1\dot{y} + k_1(x - x_0) \tag{3.6}$$

where, for $n = 2$, the displacements z and y are determined from equations (3.7) and (3.8), respectively

$$\dot{z} = -\gamma|\dot{x} - \dot{y}|z|z|^{n-1} - \beta(\dot{x} - \dot{y})|z|^n + A(\dot{x} - \dot{y}) \tag{3.7}$$

$$\dot{y} = \frac{1}{c_0 + c_1}[az + c_0\dot{x} + k_0(x - y)] \tag{3.8}$$

The residual parameters in equation (3.5), (3.6), (3.7), (3.8) denote

β, γ, A – parameters representing the control of the linearity during unloading and the smoothness of the transition from the pre-yield to post-yield region

α – parameter representing stiffness for the damping force component associated with the evolution variable z

k_0 – parameter representing the control of the stiffness of the spring at higher velocities

k_1 – parameter representing stiffness of the spring associated with the nominal damper due to the accumulator

c_0 – parameter representing viscous damping observed at higher velocities

c_1 – parameter representing the dashpot included in the model to produce the roll off at low velocities

x_0 – parameter representing the initial displacement of the spring with the stiffness k_1.

The model formulated by Spencer features high fidelity of MR damper behaviour over a wide operational range. It incorporates also the case when the acceleration and velocity have opposite signs and the magnitudes of velocities are small.

4. Experimental investigations

A linear damper of RD – 1005 series, manufactured by Lord Corporation has been investigated. The damper, developed as a replacement damper for a truck seating is a small shock absorber using an MR fluid, having a stroke of 0.054 m. Electrical and mechanical specifications of the RD – 1005 damper are as follows: max input current – 2 A, input voltage 12 VDC, resistance – 5 Ω at ambient temperature, and – 7 Ω at 71°C, damper forces $F \geqslant 2200$ N (at $\dot{x} = 0.05$ m/s, $I = 1$ A) and $F \geqslant 670$ N (at $\dot{x} = 0.02$ m/s, $I = 0$ A). The investigations have been carried out at an experimental setup with a computer-controlled INSTRON test machine of 8511.20 type. Special fixtures were designed for holding the damper in the grippers of the upper and lower machine heads properly (see. Fig. 7).

Both the piston displacement x and the damping force F have been measured with a sampling frequency of 200 Hz for one cycle (the cycle is assumed here as a full, up and down piston displacement). Piston velocity has been computed by numerical differentiation. The maximum frequency available in the tests was up to 10 Hz and the displacement amplitude up to $20 \cdot 10^{-3}$ m, and their limit values were restricted due to the efficiency of the INSTRON electro-hydraulic system. The INSTRON test machine was programmed to move up and down in a sinusoidal, triangular and trapezium wave at a certain

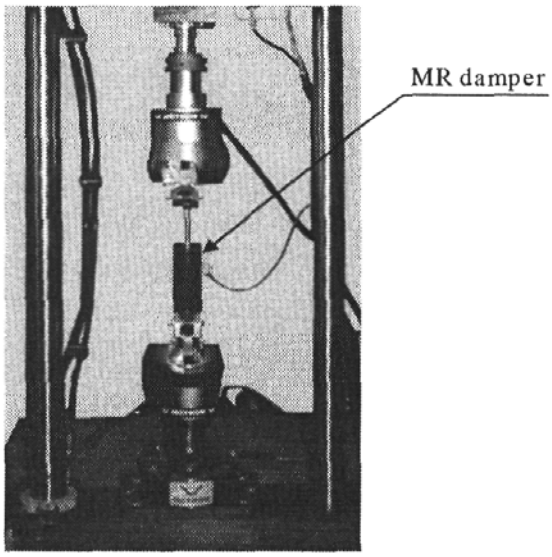

Fig. 7. MR damper of RD – 1005 type mounted in the INSTRON test machine

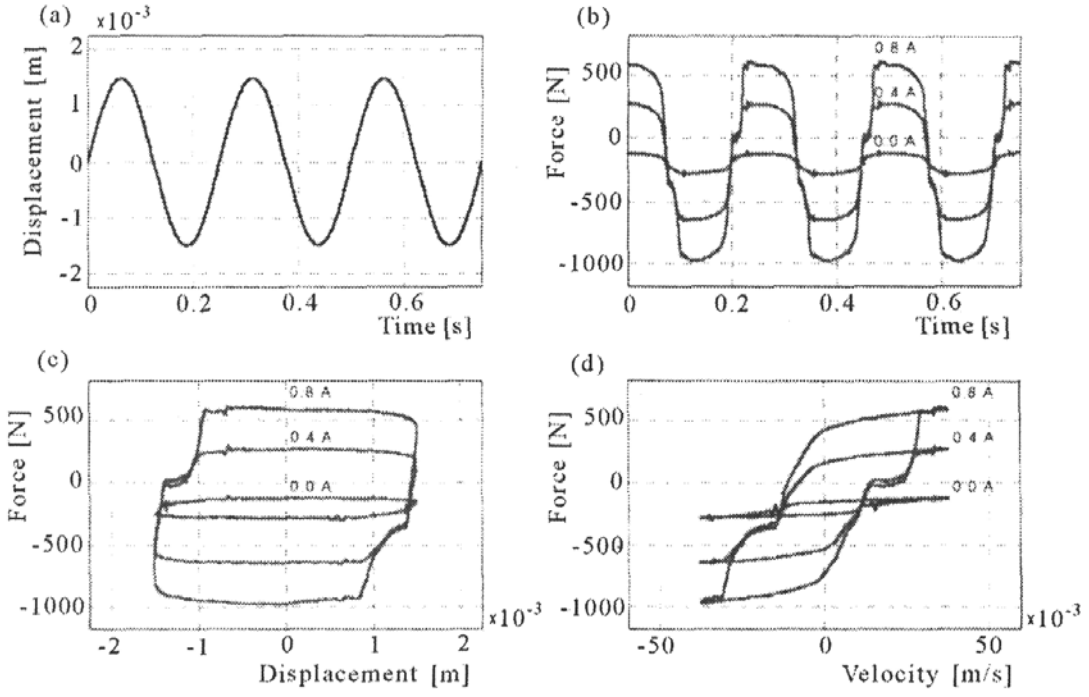

Fig. 8. Experimental relationships of: (a) sinusoidal kinematic excitation $f = 4\,\mathrm{Hz}$, $A_0 = 1.5 \cdot 10^{-3}\mathrm{m}$, (b) force vs. time, (c) force vs. displacement, (d) force vs. velocity $I = 0.0\,\mathrm{A}$, $0.4\,\mathrm{A}$, $0.8\,\mathrm{A}$

frequency and amplitude. The control current applied to the damper coil was varied within a range of $0.0 \div 1.6$ A. The experimental results obtained in the tests were given in detail by Sapiński (2001a). The exemplary ones, resulting from the sinusoidal kinematic excitation $x(t) = A_0 t \sin(2\pi f)$, ($f = 4$ Hz, $A_0 = 1.5 \cdot 10^{-3}$ m) and a control current $I = 0.0$ A, 0.4 A, 0.8 A, are shown in Fig. 8.

5. Identification of model parameters

The aim of the identification is to determine actual parameter values for the Bingham and Spencer models of the linear MR damper of RD – 1005 series. These parameters include f_c, c_0, f_0 and x_0, α, c_0, k_0, c_1, k_1, γ, β, A for the Bingham and Spencer models respectively. It has been assumed that for each kinematic excitation 20 cycles have to be examined. Cycles No. 8, 9 and 10 will be used as stable cycles of the assigned data sets (t_k, x_k), (x_k, F_k), $(\dot{x}, F_k)$, where $k = 1, ..., 600$ and x_k, $\dot{x}_k$, F_k are the piston displacement and velocity as well as damping force at the time t_k, respectively. The largest differences have been found in the data sets $(\dot{x}, F_k)$ used for examination of the excitation parameters (f, A) and control current. Such differences result primarily from numerical differentiation of the displacement vector x_k. For the identification, the results obtained for the sinusoidal kinematic excitation $x(t) = A_0 t \sin(2\pi f)$ with the following parameters ($f = 1$ Hz, $A_0 = 10 \cdot 10^{-3}$ m), ($f = 2.5$ Hz, $A_0 = 4 \cdot 10^{-3}$ m), ($f = 4$ Hz, $A_0 = 1.5 \cdot 10^{-3}$ m), and the control current I of 0.0 A, 0.4 A and 0.8 A were used. For computation of the parameters the criteria by Spencer et al. (1998) have been adopted

$$\begin{aligned} \varepsilon_t &= \int_0^T (F_e - F_m)^2 \, dt \\ \varepsilon_x &= \int_0^T (F_e - F_m)^2 \left| \frac{dx}{dt} \right| dt \\ \varepsilon_{\dot{x}} &= \int_0^T (F_e - F_m)^2 \left| \frac{d\dot{x}}{dt} \right| dt \end{aligned} \tag{5.1}$$

where F_e and F_m denote damping forces derived from the experiments and the model, respectively. The criteria define for each model the difference between F_e and F_m as a function of time $(5.1)_1$, displacement $(5.1)_2$ and velocity $(5.1)_3$.

For computation the CONSTR subroutine available in MATLAB 5.3 optimisation toolbox was employed (this subroutine is replaced with FMINCON in later versions of MATLAB/SIMULINK). The procedure finds the minimum of a function of several variables under some constrains imposed on the variables.

The following algorithm was used:

- enter the measured value of the damping force F_e for given excitation parameters f, A and control current I
- choose such initial values of the parameters so that computations could proceed quickly and properly (by checking the gradient after first iteration)
- enter parameters determined under criterion $(5.1)_1$ as the initial values for computations under criterion $(5.1)_2$, and so on
- stop the computations if a satisfactory result is reached (here: visual fit criterion).

The results of the identification obtained by the above mentioned procedure are presented in Table 1 for the Bingham model and in Table 2 and Table 3 for the Spencer model. Based on the obtained parameters theoretical relationships were established for the damping force vs. time, damping force vs. displacement and damping force vs. velocity, using MATLAB/SIMULINK 5.3 software. These relationships compared with the experimental data are shown for the Bingham model in Fig. 9 and Fig. 10 and for the Spencer model in Fig. 11 and Fig. 12. The grey lines ndicate the experimental data, while the theoretical relationships are marked with black lines.

Table 1. Parameters of the Bingham model

Current	Value of the parameter					
	$f = 1\,\mathrm{Hz},\ A_0 = 10 \cdot 10^{-3}\,\mathrm{m}$			$f = 4\,\mathrm{Hz},\ A_0 = 1.5 \cdot 10^{-3}\,\mathrm{m}$		
I [A]	f_c [N]	c_0 [N s/m]	f_0 [N]	f_c [N]	c_0 [N s/m]	f_0 [N]
0.0	44.47	3.76	−177.34	12.64	1911.40	−203.04
0.2	152.69	13.38	−173.32	64.30	4590.00	−199.12
0.4	342.05	30.53	−171.02	92.52	10301.40	−190.20
0.6	468.16	43.65	−171.78	92.76	15549.30	−187.49
0.8	538.45	51.16	−174.74	93.12	18955.20	−185.29
1.0	580.31	56.77	−176.62	92.01	21049.40	−178.94
1.2	604.24	62.71	−181.99	93.32	22637.90	−182.64
1.6	676.28	63.11	−183.01	89.26	25332.30	−184.15

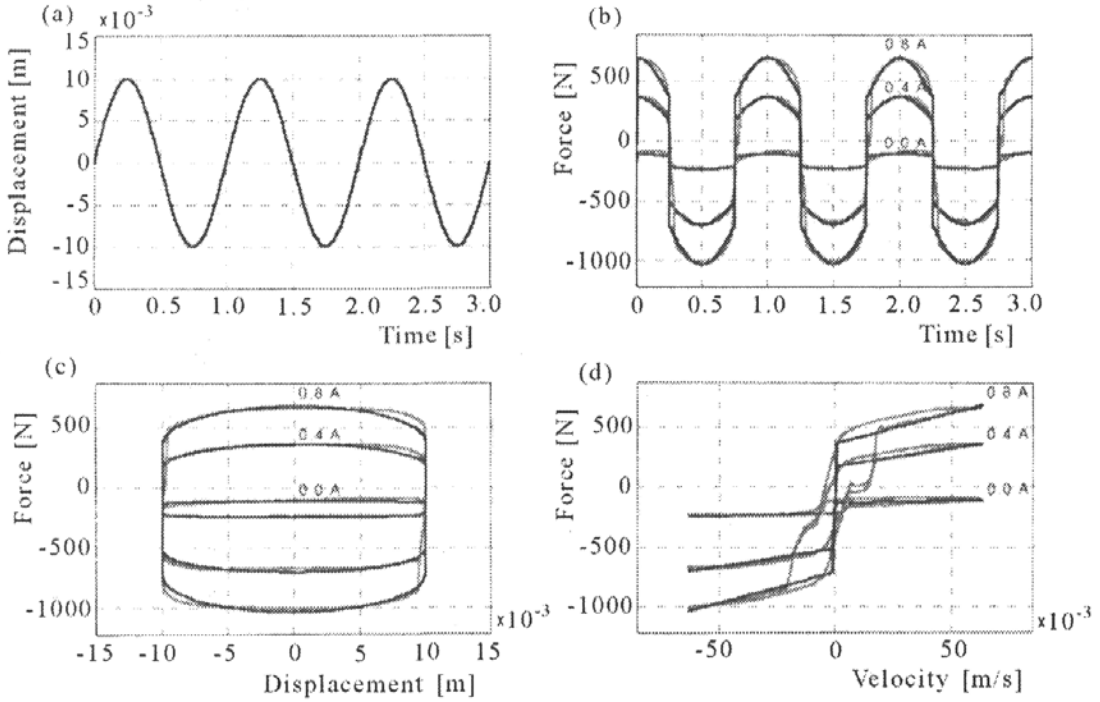

Fig. 9. Comparison of the Bingham model – predicted results with experimental data: (a) sinusoidal kinematic excitation vs. time $f = 1\,\mathrm{Hz}$, $A_0 = 10 \cdot 10^{-3}\,\mathrm{m}$, (b) force vs. time, (c) force vs. displacement, (d) force vs. velocity

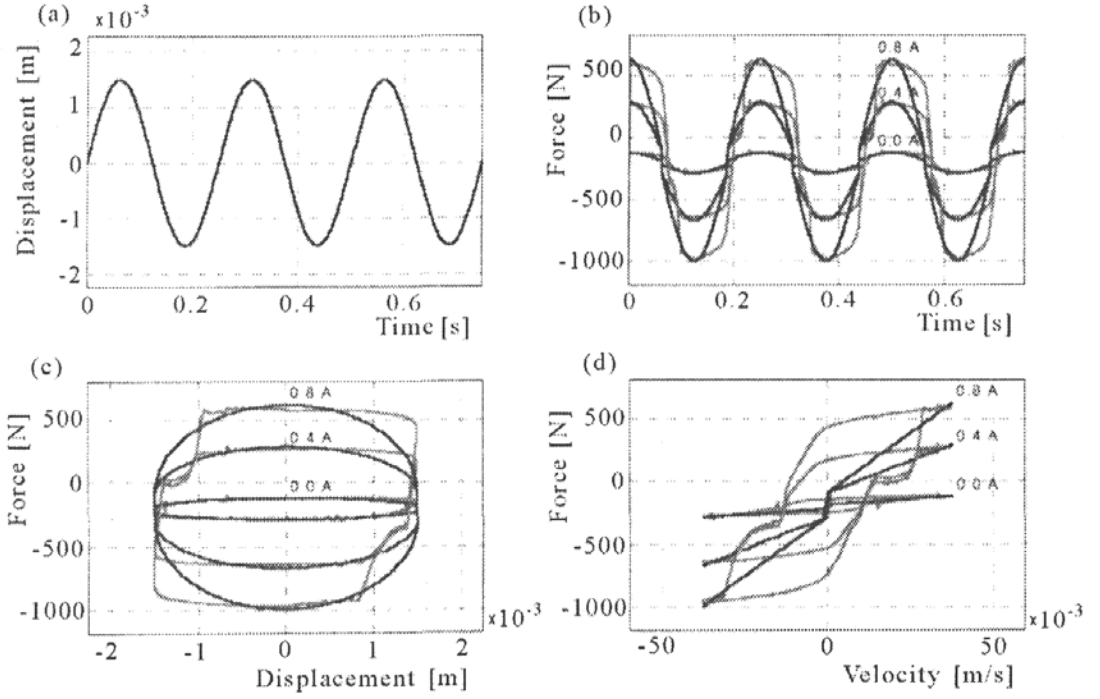

Fig. 10. Comparison of the Bingham model – predicted results with experimental data: (a) sinusoidal kinematic excitation vs. time $f = 4\,\mathrm{Hz}$, $A_0 = 1.5 \cdot 10^{-3}\,\mathrm{m}$, (b) force vs. time, (c) force vs. displacement, (d) force vs. velocity

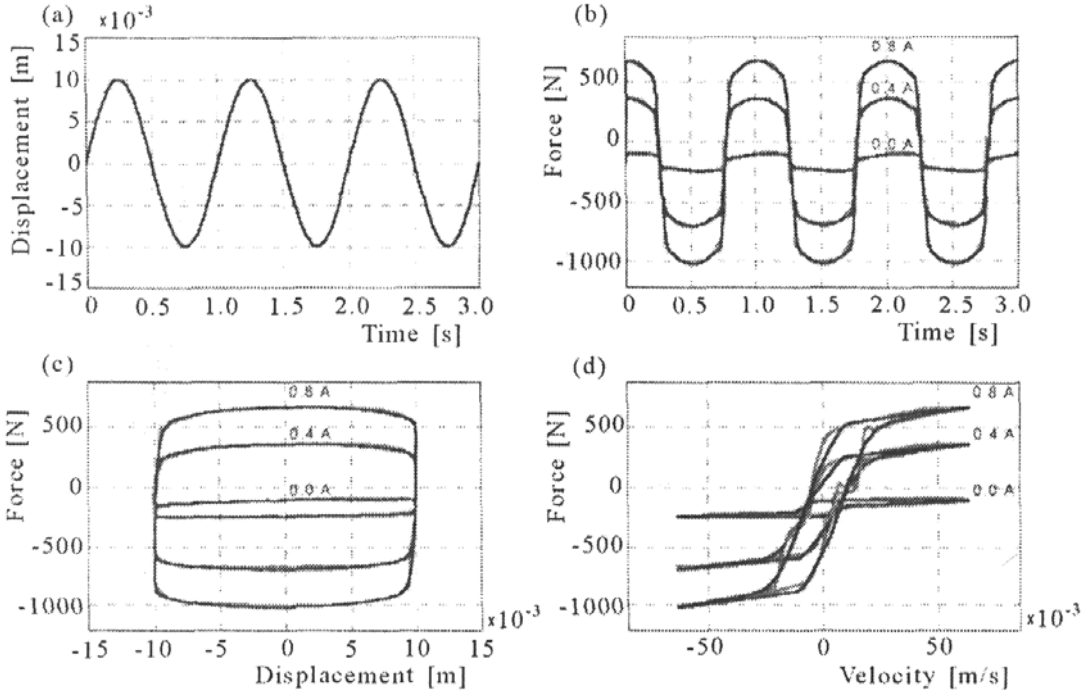

Fig. 11. Comparison of the Spencer model – predicted results with experimental data: (a) sinusoidal kinematic excitation vs. time $f = 1\,\mathrm{Hz}$, $A_0 = 10 \cdot 10^{-3}\,\mathrm{m}$, (b) force vs. time, (c) force vs. displacement, (d) force vs. velocity

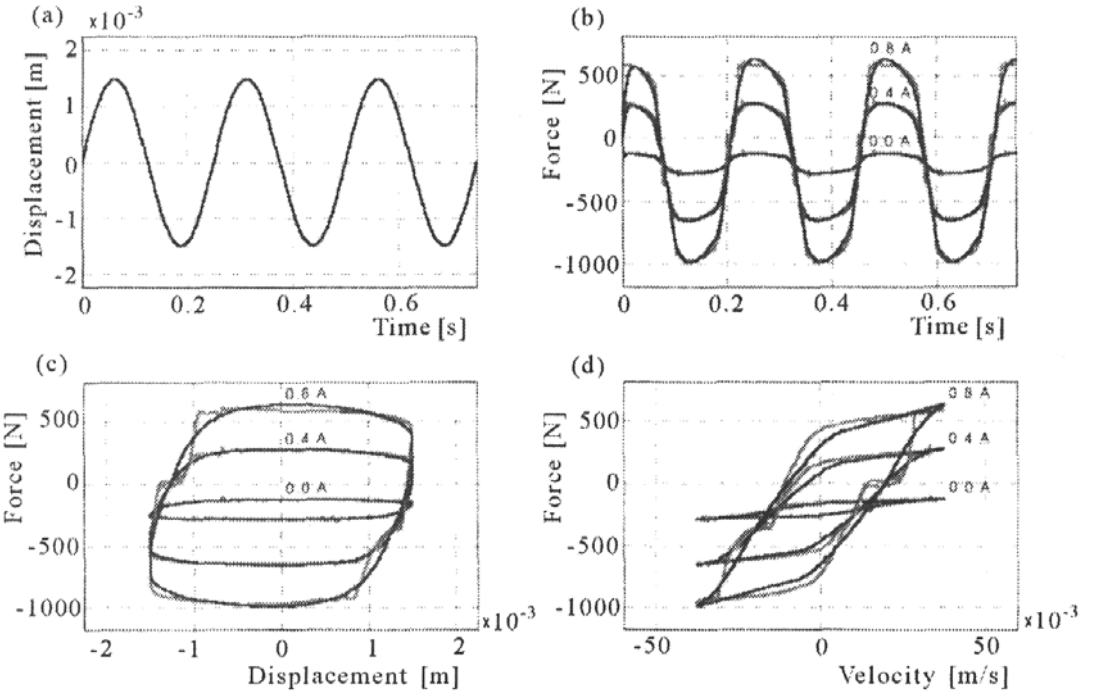

Fig. 12. Comparison of the Spencer model – predicted results with experimental data: (a) sinusoidal kinematic excitation vs. time $f = 4\,\mathrm{Hz}$, $A_0 = 1.5 \cdot 10^{-3}\,\mathrm{m}$, (b) force vs. time, (c) force vs. displacement, (d) force vs. velocity

Table 2. Parameters of the Spencer model: $f = 1\,\mathrm{Hz}$, $A_0 = 10 \cdot 10^{-3}\,\mathrm{m}$

Current	Value of the parameter				
I [A]	α [N/m]	c_0 [N s/m]	c_1 [N s/m]	k_0 [N/m]	A [–]
0.0	29870.00	348.60	69870.20	1181.60	17.66
0.2	49069.80	1138.90	33713.20	1807.10	31.68
0.4	52501.50	2138.80	38550.60	674.20	36.48
0.6	49089.90	2767.80	49329.40	1935.40	48.54
0.8	14941.10	3118.60	58017.10	2194.70	177.01
1.0	88904.50	3365.00	72971.30	1515.50	28.46
1.2	94203.30	3696.10	77044.10	1460.70	26.93
1.6	96124.60	3817.50	71696.30	359.30	33.12

Current	Value of the parameter			
I [A]	β [m^{-2}]	γ [m^{-2}]	k_1 [N/m]	x_0 [m]
0.0	3482170.00	3947050.00	705.80	0.25
0.2	420710.00	2213140.00	550.80	0.31
0.4	148340.00	422100.00	633.00	0.27
0.6	125070.00	205480.00	653.90	0.26
0.8	44220.00	38470.00	337.00	0.52
1.0	60000.00	341950.00	713.90	0.25
1.2	66880.00	315050.00	770.80	0.23
1.6	84290.00	311480.00	724.60	0.25

Table 3. Parameters of the Spencer model: $f = 4\,\mathrm{Hz}$, $A_0 = 1.5 \cdot 10^{-3}\,\mathrm{m}$

Current	Value of the parameter				
I [A]	α [N/m]	c_0 [N s/m]	c_1 [N s/m]	k_0 [N/m]	A [–]
0.0	70082.30	1013.60	12414.10	2973.40	4.04
0.2	76315.90	1838.60	48179.70	2922.80	14.80
0.4	86070.10	4010.50	50238.70	2903.40	17.15
0.6	95925.20	5386.60	65616.00	2903.40	18.73
0.8	69055.10	7713.10	76963.60	2811.90	26.76
1.0	96049.50	9273.40	80506.60	2532.30	19.95
1.2	70959.30	7350.30	77859.80	1548.00	31.21
1.6	97509.40	9200.60	70012.00	2681.00	24.02

Current	Value of the parameter			
I [A]	β [m^{-2}]	γ [m^{-2}]	k_1 [N/m]	x_0 [m]
0.0	2263070.00	5712410.00	835.40	0.24
0.2	27280.00	3058400.00	839.00	0.24
0.4	13170.00	990250.00	695.90	0.27
0.6	76610.00	561290.00	412.00	0.44
0.8	54870.00	299400.00	471.30	0.38
1.0	78970.00	350430.00	427.50	0.39
1.2	52340.00	209620.00	642.80	0.27
1.6	94270.00	208440.00	285.50	0.59

6. Verification of models

The results have been verified by comparing the experimental damper response with that calculated from the identified models for triangle and trapezium excitations (thus independent of the excitation used for the identification purposes). The visual fit criterion was employed. Examples of the results obtained for the triangle excitation $f = 4\,\text{Hz}$, $A_0 = 1.5 \cdot 10^{-3}\,\text{m}$ and control current I of 0.0 A, 0.4 A and 0.8 A are shown in Fig. 13 and Fig. 14 for the Bingham and Spencer models, accordingly.

7. Conclusions

Two linear MR damper parametric models by Bingham and Spencer have been reviewed. The first one is an idealized viscoplastic model, and as the simplest, is often applied in response analysis. The second one is a high fidelity model and therefore adequate to characterize MR damper behaviour for analysis and control design and applications. The parameters of these two parametric models, which are f_c, c_0, f_0 and x_0, α, c_0, k_0, c_1, k_1, γ, β, A for the Bingham and Spencer model, respectively, have been estimated using the standard visual compatibility criterion. For this purpose a linear MR damper of RD – 1005 series under sinusoidal, triangular and trapezium excitations in the range of frequency $0.5 \div 8\,\text{Hz}$ and under a constant control current condition was experimentally tested. The range of the experimental investigations

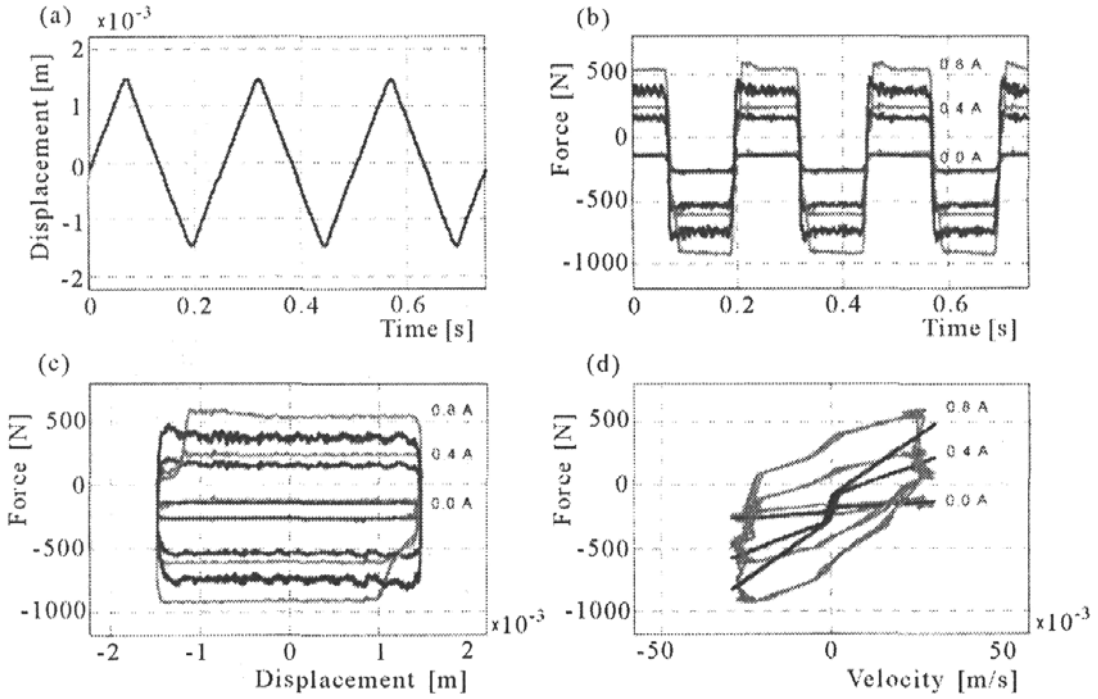

Fig. 13. Comparison of the Bingham model – predicted results with experimental data: (a) triangulal kinematic excitation vs. time $f = 4\,\mathrm{Hz}$, $A_0 = 1.5 \cdot 10^{-3}\,\mathrm{m}$, (b) force vs. time, (c) force vs. displacement, (d) force vs. velocity

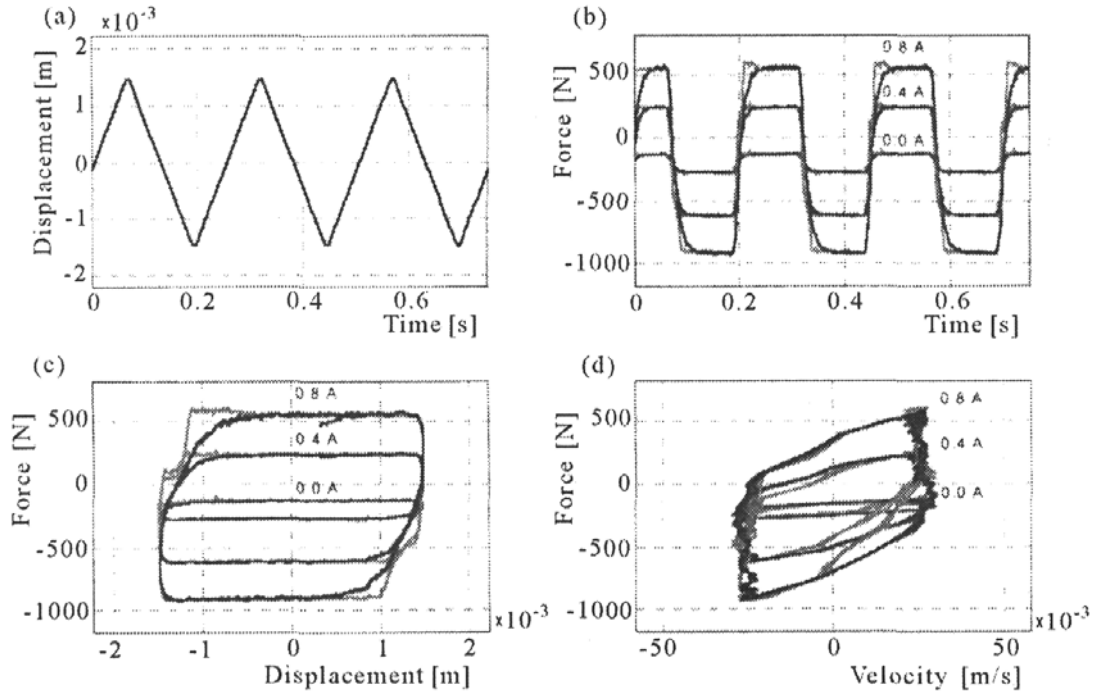

Fig. 14. Comparison of the Spencer model – predicted results with experimental data: (a) triangulal kinematic excitation vs. time $f = 4\,\mathrm{Hz}$, $A_0 = 1.5 \cdot 10^{-3}\,\mathrm{m}$, (b) force vs. time, (c) force vs. displacement, (d) force vs. velocity

was restricted at higher frequencies because of the efficiency of INSTRON electro-hydraulic system.

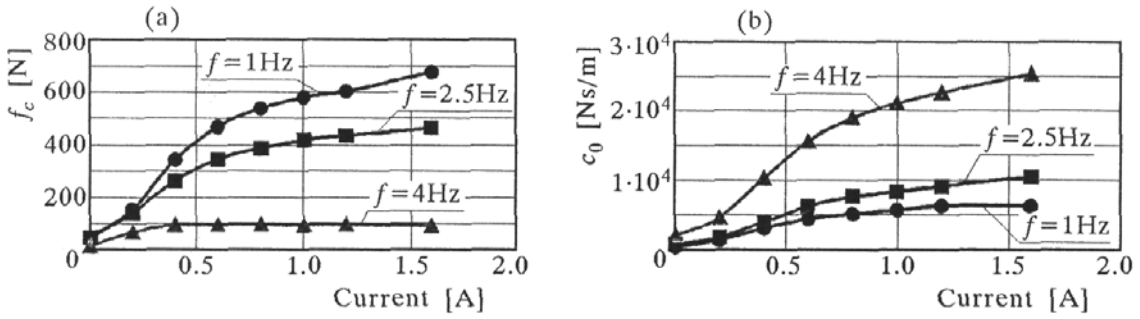

Fig. 15. The relationships of parameters of the Bingham model: (a) f_c vs. current, (b) c_0 vs. current

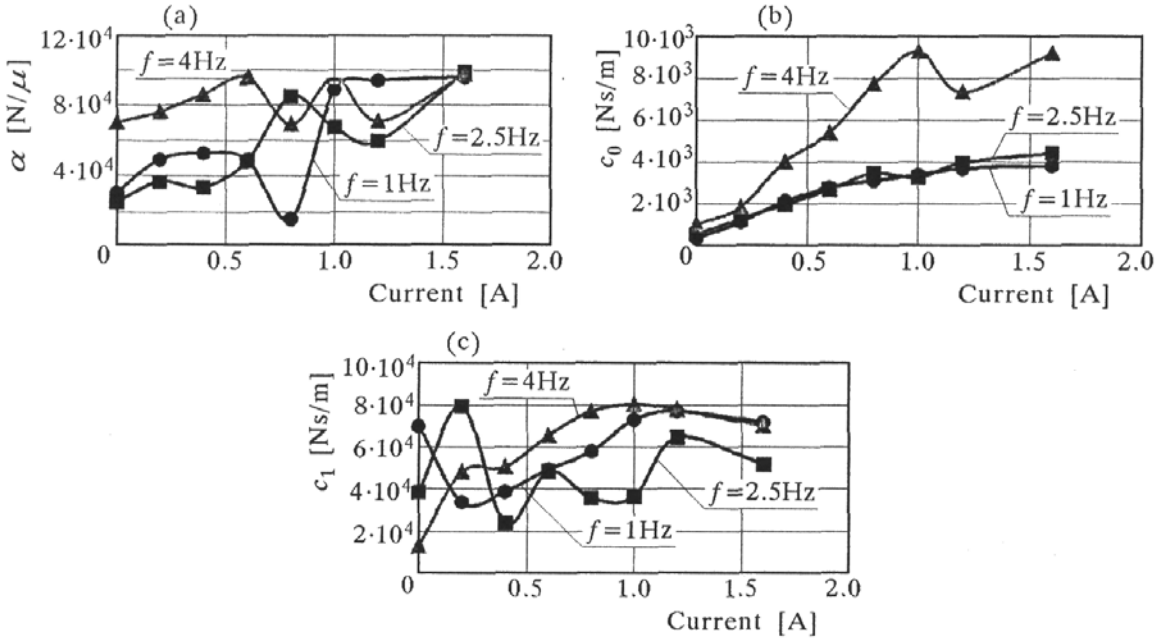

Fig. 16. The relationships of parameters of the Spencer model: (a) α vs. current, (b) c_0 vs. current, (c) c_1 vs. current

The following statements result from the carried out investigations:

- excitation frequency (amplitude) and control current strongly depend on values of certain parameters of the model
- higher capability of the Spencer model to exhibit variety of hysteric responses when compared to the Bingham one, however, in both cases several deviations from experimental data still persist

- these deviations result from nonlinear behaviour of the MR fluid under operating conditions
- no unstable cycles (Li et al., 2000) up to the frequency of 8 Hz have been observed under experimental testing
- assumption of a difference between the model-predicted damping force F_m and the experimental one F_e as the objective function to be minimized (Li et al., 2000) is not a sufficient criterion for the model parameter identification due to force vs. time, force vs. displacement, and force vs. velocity relationships
- thus, criteria $(5.1)_2, 3$ seem to be dominating in parametric identification
- fitting of the model-predicted and the experimental data becomes more appropriate with decrease in the excitation frequency
- this fitting is better for the Spencer than for the Bingham one (see Fig. 13 and Fig. 14), however at lower frequencies is quite satisfactory for both models
- the linear relationship between the parameters α, c_0, c_1 and the control current (Spencer et al., 1998) seems to be questionable for the Spencer model (see Fig. 16)
- this relationship is more suitable for the parameters of f_c, c_0 of the Bingham model (see Fig. 15).

The final confirmation of the assumption that the identified model of the MR damper adequately represents actual behaviour over a wide range of operating conditions could provide a useful tool for a control system design. If so, such a model may be effectively incorporated to the development of the control algorithm.

The model deviations observed at higher frequencies have shown that the modelling approach proposed by Spencer should be extended to viscoelastic-plastic mechanisms (Li et al., 2000), however, the investigated MR damper was designed to operate in the post-yield region, at lower frequencies with medium or high amplitudes.

Acknowledgement

The research work has been supported by the State Committee for Scientific Research as a part of the grant No. 8T07B 03520

References

1. AHMADIAN M., 1999, A non parametric model for magnetorheological dampers, *Proc. ASME Design Engineering Technical Conferences*, 1-10
2. CARLSON J.D., SPRONSTON J.L., 2000, Controllable fluids in 2000 status of ER and MR fluid technology, *"Actuator 2000" – 7th International Conference on New Actuators*
3. CHANG C.C., ROSCHKE P., 1998, Neural network modeling of a magnetorheological damper, *Journal of Intelligent Material Systems and Structures*, **9**, 755-764
4. DYKE S., SPENCER B., SAIN M., CARLSON J., 1996, Phenomenological model of a magnetorheological damper, *Journal of Engineering Mechanics*
5. GRZESIKIEWICZ W., KNAP L., LASSOTA W., MARZEC Z., 1999, Identyfikacja modelu magnetoreologicznego tłumika drgań, *Materiały IV Szkoły – Metody Aktywne Redukcji Drgań i Hałasu*, 83-88
6. KAMATH G.M., WERELY N.M., 1997, Nonlinear viscoelastic – plastic mechanisms based model of an electrorheological damper, *Journal of Guidance, Control and Dynamics*, **6**, 1125-1132
7. KORDONSKI W., 1993, Elements and devices based on magnetorheological effect, *Journal of Intelligent Systems and Structures*, **4**, 65-69
8. LEDERER P., SALLOKER M.G., DOCZY S., 2000, Modelling of a magnetorheological damper by parameter estimation, *7th International Conference on New Actuators*, 143-146
9. LI W.H., YAO G.Z., CHEN G., YEO S.H., YAP F.F., 2000, Testing and steady state modelling of a linear MR damper under sinusoidal Loading, *Smart Materials and Structures*, **9**, 95-102
10. SAPIŃSKI B., 2001a, Badania eksperymentalne charakterystyk mechanicznych liniowego tłumika magnetoreologicznego, *Materiały V Szkoły – Metody Aktywne Redukcji Drgań i Hałasu*, 257-268
11. SAPIŃSKI B., 2001b, Wpływ fluktuacji pola magnetycznego na charakterystyki mechaniczne liniowego tłumika magnetoreologicznego, *Zeszyty Naukowe Politechniki Krakowskiej, Mechanika*, **83**, 243-252
12. SCHURTER K.C., ROSCHKE P.N., 2000, Fuzzy modeling of a magnetorheological damper using ANFIS, *Proc. 9th IEEE International Conference on Fuzzy Systems*, 122-127
13. SODERSTROM T., STOICA P., 1997, *Identyfikacja systemów*, PWN, Warszawa
14. STANWAY R., SIMS N.D., JOHNSON A.R., 2000, Modelling and control of a magnetorheological vibration isolator, *Smart Structures and Materials 2000: Damping and Isolation, Proc. of SPIE*, **3989**, 184-192

15. SPENCER B.F. JR., YANG G., CARLSON J.D., SAIN M.K., 1998, Smart dampers for seismic protection of stuctures: a full-scale study, *Proc. 2nd World Conference on Structural Control*

16. SUNAKODA K., SODEYAMA H., IWATA N., FUJITANI H., SODA S., 2000, Dynamic characteristics of magnetorheological fluid damper, *Smart Structures and Materials: Damping and Isolation. Proc. of SPIE*, **3989**, 194-202

17. WEN Y., 1976, Method for random vibration of hysteretic systems, *Journal of The Engineering Mechanics Division*, 249-263

Identyfikacja parametryczna małogabarytowego liniowego tłumika MR

Streszczenie

W artykule przedstawiono problem identyfikacji parametrycznej modeli fenomenologicznych liniowego tłumika magnetoreologicznego (MR). Rozważono struktury reologiczne tłumika MR opisane modelami Binghama i Spencera. Sformułowano zadanie identyfikacji, pokazano przykładowe wyniki badań doświadczalnych tłumika oraz procedurę doboru estymowanych współczynników modeli odpowiadających danym uzyskanym z eksperymentu identyfikacyjnego. Obiektem badań był małogabarytowy tłumik MR, typu RD-1005 wyprodukowany przez firmę Lord Corporation.

Manuscript received November 15, 2001, accepted for print March 4, 2002